

## Organic-inorganic mesoporous silica nanostrands for ultrafine filtration of spherical nanoparticles

Sherif A. El-Safty, Moataz Mekawy, Akira Yamaguchi, Ahmed Shahat, Kazuyuki Ogawa, and Norio Teramae

### Supplementary (S1)

#### S1.1. Synthesis of organic-inorganic mesoporous hybrid AAM

In typical conditions, anhydrous toluene (10 ml) solutions containing (3 ml) trimethylchlorosilane (TMCS) and the calcined silica NSs hybrid AAM were refluxed at 80–100 °C for 24 h, under N<sub>2</sub> atmosphere. A 5 ml of dehydrated pyridine was added to the refluxed mixture to remove the resultant Cl<sup>-</sup> anions. The total mixture was then refluxed 60 °C for 24 h. The reaction mixture was washed thoroughly with cyclohexane and acetone to remove the unreacted TMCS. Of these grafting techniques, layered surface chemistry was achieved inside the pore channel by means of a series of dense silanization cycles used to graft TMS to the silica NSs grown in the AAM membranes.

<sup>29</sup>Si nuclear magnetic resonance (NMR) spectra (Fig. S1 ESI†) of silica and TMS-silica strands show two main resonance peaks at -110.1 ppm and at -101 ppm, as well as a weak peak at -92 ppm. These three peaks correspond to Si(OSi)<sub>4</sub> (Q<sub>4</sub>), (HO)Si(OSi)<sub>3</sub> (Q<sub>3</sub>) and (HO)<sub>2</sub>Si(OSi)<sub>2</sub> (Q<sub>2</sub>) silicate species, respectively. With incorporation of TMS groups into the silica NTs, the Q<sub>3</sub> peak decreased substantially, and a new peak (T<sub>1</sub>) appeared at 13 ppm due to silicon bonded to the TMS. Moreover, the increase in the intensity of the siloxane groups' peak (Q<sub>4</sub>) indicates that Si–OH sites (corresponding to silanediol and silanol groups) in the inner pores of the silica strands underwent condensation with TMS, thus forming covalent linkages to the silica framework. The sharp signal of (M<sub>1</sub>) corresponds to the main component of the hydrophobic TMS silane, indicating that TMS molecules were located in close proximity of each other in a well-defined monolayer rather than a polymerized random multilayer.

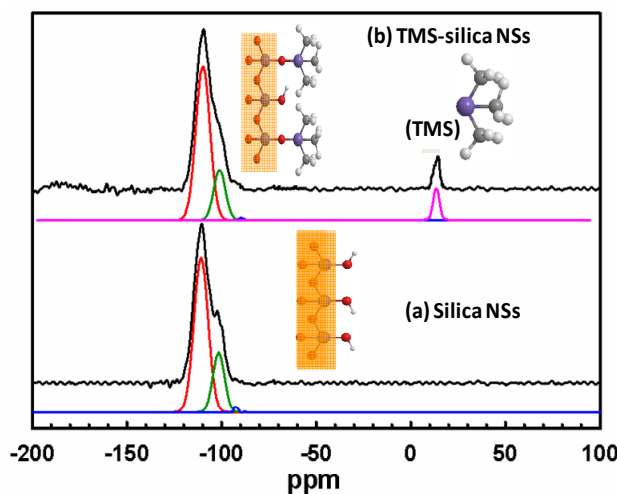


**Fig. S1.1.** <sup>29</sup>Si MAS NMR spectra and a deconvolution of each spectrum of silica and TMS-modified silica NSs via direct, dense silanization cycles of TMCS.

## Supplementary (S2)

### S2. 1. SAXS and N<sub>2</sub> isotherms of nanostrands

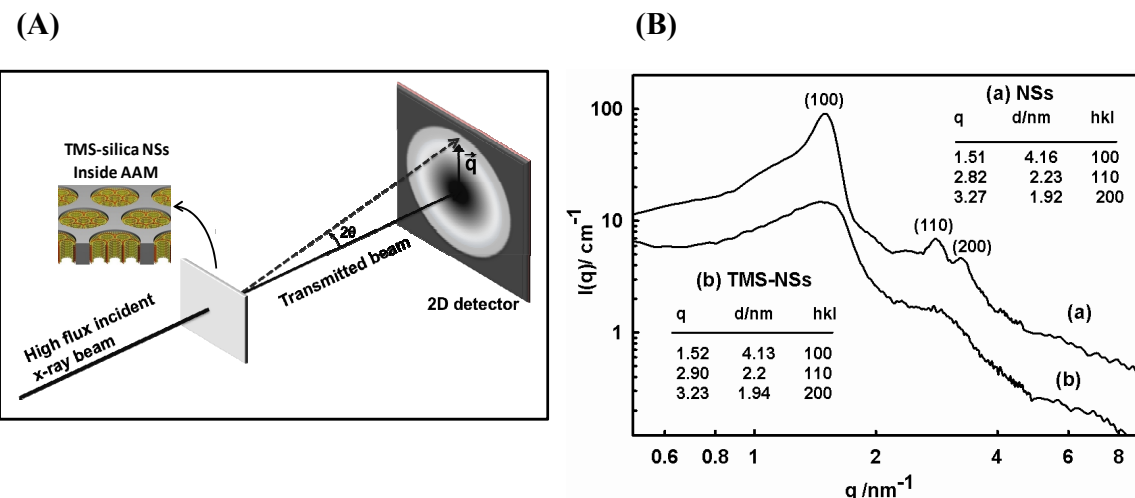


**Fig. S2.1.** The SAXS geometry of the present work (A). SAXS patterns (B) of hexagonal mesoporous silica (a) and TMS-silica (b) NSs that fabricated inside the AAM membrane using CTAB surfactant as structural-directing agent. The 2D SAXS patterns were recorded by 2D detector (Bruker High-star) covering a range of momentum transfer  $q = (4\pi / \lambda) \sin(2\theta/2)$ , from 0.2 to 10 cm<sup>-1</sup>, where  $\lambda$  is wavelength of the incident x-ray beam and the  $2\theta$  is the scattering angle.

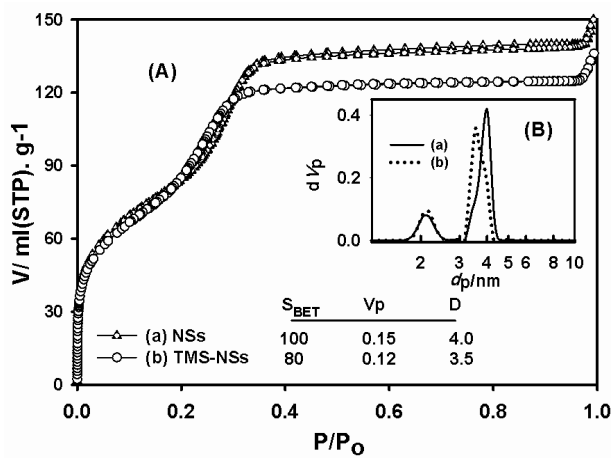


**Fig. S2.1.**  $N_2$  isotherms (A) & NLDFT pore-size distribution (B) of mesoporous silica (a) and TMS-silica (b) NSs that fabricated inside the AAM membrane using CTAB surfactant as structural-directing agent. Inserts: BET surface area ( $S/\text{m}^2 \cdot \text{g}^{-1}$ ), pore volume ( $V_p/\text{cm}^3 \cdot \text{g}^{-1}$ ) and NLDFT pore size distribution ( $D/\text{nm}$ ).  $N_2$  isotherms were measured using a BELSORP MIN-II analyzer (JP. BEL Co. Ltd) at 77 K. The pore size distribution was determined from the adsorption isotherms by using nonlocal density functional theory (NLDFT). These results revealed that TMS-silica NSs retained the textural features (i.e.,  $S_{\text{BET}}$  and  $V_p$ ) noted above for the uncoated silica. However, the TMS-silica strands retained ~80% of their original surface area and pore volume, thus leading to efficient separation system.

## **Supplementary (S3)**

### **S3.1. Synthesis of NM NPs and SC NCs**

#### **Synthesis of Ag NPs:**

In typical one-step synthesis, a 1 mmol  $\text{AgNO}_3$  was dissolved in 30 ml deionized water, then 0.3–1.5 mmol CTAB was put into the solution; the solution turned yellow because of the formation of  $\text{AgBr}$ . After stirring for 10 min, 10 ml 0.2 M ascorbic acid was added into the above solution, and then it was transferred to a 55 ml Teflon-lined autoclave. The final concentrations of  $[\text{Ag}^+]$  and  $[\text{CTAB}]$  were 0.025 M, and 0.0075 M. The hydrothermal was carried out at 160°C for ~16 h. The powders were collected and washed in ID water and ethanol several times by centrifuging at 3000 RPM, then dry at 45°C.<sup>16a</sup>

#### **Synthesis of CdS NCs:**

The mixture of 0.55 ml dodecanethiol and 0.2 g  $\text{CdCl}_2$  (in the molar ratio of 2.5:1) was stirred for 10 minute. The solution was transferred to a Teflon-lined autoclave sealed and heated at 160°C for several hours. After reaction, the solid CdS NCs were washed in ID water and ethanol several times and collected by centrifuging at 3000 RPM, and then dry at 45°C.<sup>16b</sup>

#### **Synthesis of Au & Pt nanoparticles:**

A mixture of 40 mg  $\text{AuCl}_3$ , and 1g oleylamine were dissolved in 10 ml chloroform with stirred for 2h at 60°C. To this mixture composition, a 20 ml acetone was added to precipitate the Au nanoparticles. The precipitated Au nanoparticles were then collected and thoroughly washed with ID water and ethanol by means of a centrifuge. The Au NPs were then dried at 45°C in air. Synthesis of Pt nanoparticles with octadecylamine followed the same procedures; however, the Pt compound of dipotassium hexachloroplatinum ( $\text{K}_2\text{PtCl}_6$ ) was used as Pt source.<sup>16c</sup>

Note that within the filtration assay, the precipitated particles were dispersed in chloroform (2 mL).

#### **S3.2.1. Ultrafine filtration of Ag NPs**

The HR-TEM images show highly crystalline Ag NPs with clearly cubic lattice crystallography for their *fcc* phases. However, the electron diffraction (ED) patterns (Fig. 3Aa and 3Ba) clearly show six-ring patterns, which indicate d-spacing ratios of  $\sqrt{3}$ ,  $\sqrt{4}$ ,  $\sqrt{8}$ ,  $\sqrt{11}$ ,  $\sqrt{12}$  and  $\sqrt{19}$ , corresponding to the [111], [200], [220], [311], [222] and [331] reflections of cubic *Fm̄3m* space of the Ag NPs. In turn, a magnified HR-TEM image of filtered Ag NPs revealed high crystallinity, which agrees with the presence of *fcc* lattices in the Ag NPs.

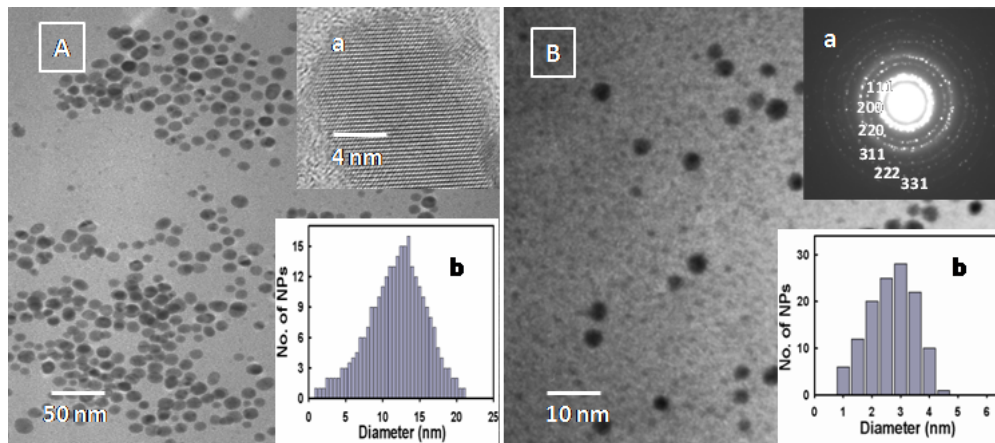


**Fig. S3.2.1 A** HR-TEM micrographs of Ag NPs before (A) and after (B) ultra-fine separation assay by TMS-silica NSs hybrid membranes. Inserts (A) are high-magnification TEM of one Ag NP (a) and histogram of Ag NPs patterns (b). Inserts (B) are the ED (a) and histograms (b) of highly ordered AgNPs arrays with *fcc* phase of cubic *Fm̄3m* symmetry that produced after applying the ultra-fine separation assay, respectively.

#### **S3.2.1. XRD characterization of NPs and NCs with noble and semiconductor metals**

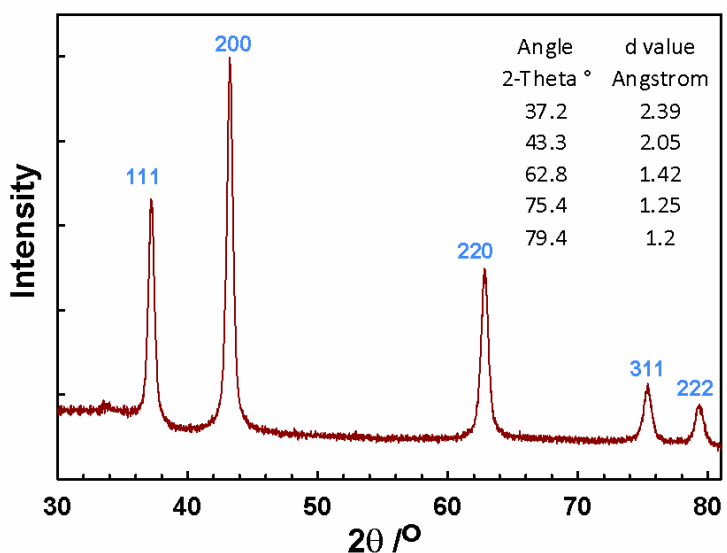


**Fig. S3.2A** XRD pattern of spherical Ag nanoparticles with cubic Fm<sub>3</sub>m structure. Inserts are the assignment of the high intensity reflection peaks.

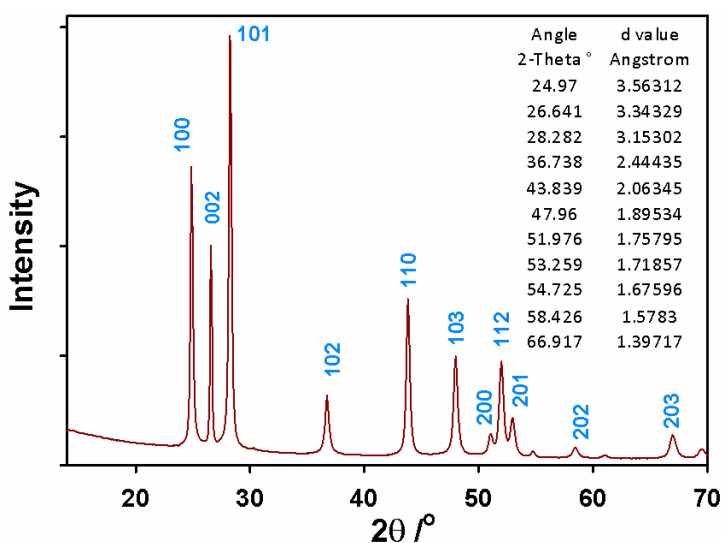


**Fig. S3.2.B** XRD pattern of Pyramidal/spherical CdS nanocrystals with hexagonal P<sub>6</sub><sub>3</sub>/mmc (*hcp*) structure. Inserts are the assignment of the high intensity reflection peaks.

## **Supplementary (S4)**

### **S4.1. Ultrafine filtration of cytochrome c**

Within the separation systems of cytochrome c, the TMS-silica NSs inside 1D AAM membrane (Whatman International Ltd., England; with diameter of 2.5 cm) was fixed in an ordinary filtration apparatus, which connected with vacuum pump at pressure  $\leq 0.01$  MPa and at room temperature. To this membrane, A 5 mL of protein solution was dropped. The successful separation of large quantity of cytochrome c protein was occurred in very fast separation time (in seconds). The aliquot cytochrome c was studied by monitoring the change in absorbance at 409 nm for cytochrome c using UV-vis spectroscopy (Fig. S4). The filtration assay illustrates that 92 % of cytochrome c was filtrated from the feed solution in 10 seconds, as evidenced from the decrease of the absorbance at the specific wavelength.

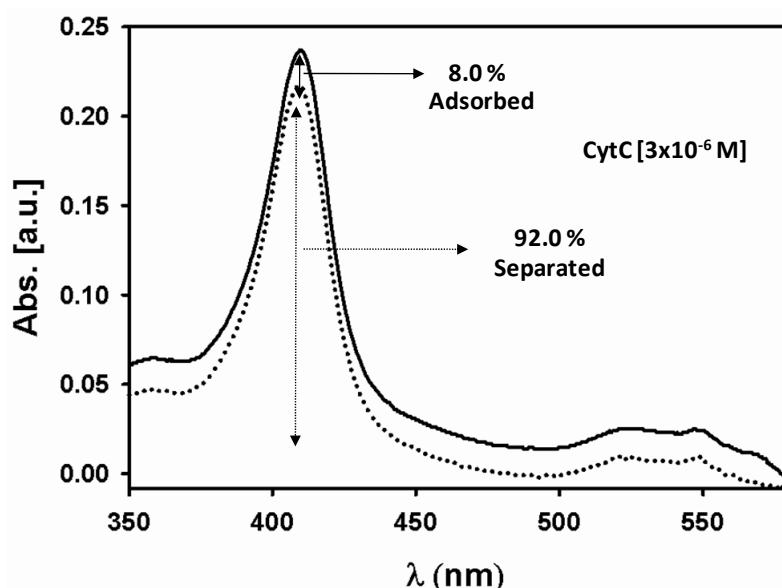


**Fig. S4** Absorbance spectra corresponding to  $[3 \times 10^{-6}$  M] of cytochrome c (CytC) before (solid-line) and after (dotted-line) ultra-fine separation assay.